Testing axial and electromagnetic nucleon form factors in time-like regions in the processes $\bar{p} + n \to \pi^- + \ell^- + \ell^+$ and $\bar{p} + p \to \pi^0 + \ell^- + \ell^+, \ell = e, \mu$

C. Adamuščín,[*] E. A. Kuraev,[†] and E. Tomasi-Gustafsson[‡]
DAPNIA/SPhN, CEA/Saclay, F-91191 Gif-sur-Yvette Cedex, France

F. E. Maas
CNRS/INP3, IPN Orsay, F-91400 Orsay Cedex, France
(Received 1 November 2006; published 20 April 2007)

In the frame of a phenomenological approach based on Compton-like Feynman amplitudes, we study the annihilation channel in antiproton nucleon collisions with production of a single charged or neutral pion and a lepton-antilepton pair. These reactions allow us to access nucleon and axial electromagnetic form factors in the time-like region and offer a unique possibility to study the kinematical region below the two-nucleon threshold. The differential cross section in an experimental setup where the pion is fully detected is given with explicit dependence on the relevant nucleon form factors. The possibility of measuring a heavy charged pion in the annihilation channel is also discussed.

DOI: 10.1103/PhysRevC.75.045205 PACS number(s): 25.43.+t, 12.40.Vv, 13.40.Gp, 13.75.Gx

I. INTRODUCTION

In this paper we study the annihilation reactions $\bar{p} + n \to \pi^- + \ell^- + \ell^+$ and $\bar{p} + p \to \pi^0 + \ell^- + \ell^+, \ell = e, \mu$, which is the crossed process of pion electroproduction on a nucleon N: $e^- + N \to e^- + N + \pi$. It contains the same information on the nucleon from factors in a different kinematical region. This process is also related to the pion scattering process $\pi + N \to N + \ell^- + \ell^+$, which was first studied in Ref. [1]. In this work it was already pointed out that the $\bar{p} + p$ annihilation process with pion production, under study here, renders possible the determination of the nucleon electromagnetic form factors in the unphysical region, which is otherwise unreachable in the annihilation reaction $\bar{p} + p \to e^+ + e^-$. In Ref, [2] a general expression for the cross section was derived and numerical estimations were given in the kinematical region near threshold. In this paper we extend the formalism in two directions. We take into account a larger set of diagrams that can contribute and give special emphasis to the possibility of accessing the axial nucleon form factors in the time-like region. For the annihilation process $\bar{p} + N \to \ell^+ + \ell^- + \pi^{0,-}$, with $\ell = e$ or μ, we will consider two reactions:

$$\bar{p}(p_1) + p(p_2) \to \pi^0(q_\pi) + \ell^+(p_+) + \ell^-(p_-) \qquad (1)$$

and

$$\bar{p}(p_1) + n(p_2) \to \pi^-(q_\pi) + \ell^+(p_+) + \ell^-(p_-), \qquad (2)$$

where the notation of the particle four-momenta is indicated in brackets. Interest in these processes lies in the possibility of accessing nucleon and axial form factors (FFs) in the time-like region. The expected values of the total cross sections at energies of a few GeV drop with the lepton pair invariant mass, q^2, but they are of the order of several nb and up to mb below threshold. Therefore these reactions are especially interesting as they will be measurable in the near future at hadron colliders (or at lepton colliders for the crossed reactions). The present work aims to evaluate the differential cross section for experimental conditions achievable at the future FAIR facility [3].

A. Electromagnetic (vector) form factor

The structure of the proton and the nucleon is of great interest since it explores the quantum field theory of the strong interaction, quantum chromodynamics (QCD), in a region where the interaction between the constituents of quarks and gluons cannot be treated as a perturbation. Its properties have been explored in many observables. For example, the electromagnetic form factors of the proton and the nucleon are measured in elastic electron-nucleon scattering with a space-like four-momentum transfer $q^2 < 0$ via the process $e + p \to e + p$ [4]. For a momentum transfer of $-1 < q^2 < 0$ GeV^2, the electromagnetic form factors are well known for both the neutron and the proton [5].

Interest in the form factors of the nucleon for the region of $q^2 < -1$ GeV^2 has recently been renewed by a measurement of the ratio of the electric form factor over the magnetic from factor, $\mu_p G_E/G_M$, at TJNAF in a q^2 range up to -5.8 GeV^2. The method of polarization transfer [6] was employed for the first time at high values of q^2 by using a longitudinally polarized electron beam and measuring the polarization of the recoil proton [7]. The experiments gave the surprising new result that the ratio $\mu_p G_E/G_M$ decreases from unity substantially for high q^2 values, exhibiting eventually even a zero-crossing around $q^2 \approx -8$ GeV^2. This new result contrasts with the data obtained from a Rosenbluth separation fit of unpolarized measurements [8], which give a ratio of $\mu_p G_E/G_M \approx 1$. The present understanding of this

[*]Present address: Department of Theoretical Physics, IOP, Slovak Academy of Sciences, Bratislava, Slovakia.
[†]Present address: JINR-BLTP, 141980 Dubna, Moscow region, Russian Federation.
[‡]Electronic address: etomasi@cea.fr

discrepancy is that the analysis of the unpolarized data lacks important corrections stemming from neglected higher order radiative corrections [9] or electromagnetic processes such as two-photon exchange [10].

The situation of the experimental determination of the electromagnetic form factors in the time-like domain (i.e., $q^2 > 0$) is quite different. Existing data have explored the two basic processes: $e^- + e^+ \to p + \bar{p}$ and $p + \bar{p} \to e^- + e^+$. The precision of the cross-section data in the time-like region is much lower and a determination of the individual electric and magnetic form factors has not been done with sufficient precision.

For both processes there is a threshold in q^2 for producing the two nucleons at rest or annihilation of the two nucleons at rest, which amounts to $q^2 > (m_p + m_{\bar{p}})^2 = 4m_p^2$. In the region of $0 < q^2 < 4m_p^2$ (sometimes called the "unphysical region") there are no data available. Nonetheless, this q^2 interval is of great interest since the intermediate virtual photon as well as the $\bar{p}p$ pair can couple to vector meson and $\bar{p}p$ resonances, respectively, and thereby enhance the form factors substantially [11,12]. This mechanism has been used to explain the large cross section in the time-like region above the threshold $q^2 > 4m_p^2$. Another possibility for explaining this large cross section above threshold has been proposed recently by showing that the large cross section in the annihilation process $\bar{p} + p \to e^+ + e^-$ can be related to the $\bar{p}p$ scattering length [13].

The work presented here is focused on a possibility of extracting the electromagnetic form factors of the nucleon in the "unphysical region" and above by using the process $\bar{p} + p \to \pi + e^+ + e^-$, as has been proposed earlier [1,2]. The measurement of the cross section of this reaction will be accessible at the future FAIR facility at GSI.

B. Axial form factor

In addition, we explore here also the new idea of accessing the axial vector current of the nucleon. The axial form factors in the space-like region are measured in nuclear β decay, in neutrino scattering, in muon capture, and in pion electroproduction ($e + p \to e + n + \pi^+$). A review of the present status of the axial structure of the nucleon in the space-like region is given in Ref. [14]. The first methods represent a rather direct measurement in the sense that the axial coupling of the weak charged currents is used to measure the axial form factor. The extraction of the axial form factor from pion electroproduction in the space-like region is possible because of the application of a chiral Ward identity referred to as the Adler-Gilman relation [15]. A recent review on the theoretical development can be found in Ref. [16]. Corrections to $\mathcal{O}(p^4)$ have been calculated in the framework of chiral perturbation theory (ChPT) in Ref. [17]. There are no data available on the axial form factor in the time-like region. A direct measurement would be possible by studying the weak neutral or charged current in the annihilation of $\bar{p}p$. Such a measurement is not accessible with present-day experimental techniques. However, an application of the Adler-Gilman relation to the matrix element of the crossed channel of pion electroproduction, namely $\bar{p} + n \to \pi^- + e^+ + e^-$, renders the possibility of accessing the axial current also in the time-like region around and below threshold. Despite the theoretical uncertainties—namely, the applicability range of the Adler-Gilman relation, which is strict only at the π threshold, and the treatment of the off-shell nucleon between the π vertex and the virtual photon vertex—the measurement of the cross section in $\bar{p} + n \to \pi^- + e^+ + e^-$ at low energies would render the first estimation of the axial form factor in the time-like region. The measurement of the cross section of this reaction will also be accessible at the future FAIR facility at GSI.

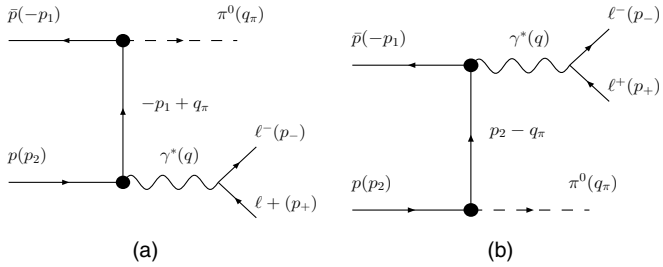

FIG. 1. Feynman diagrams for the reaction $\bar{p} + p \to \pi^0 + \ell^+ + \ell^-$.

C. Approach

Our approach is based on Compton-type annihilation Feynman amplitudes and aims to establish the matrix element of processes (1) and (2). The main uncertainty in our description in terms of Green functions of mesons and nucleons (and their expected partners) is related to the model-dependent description of hadron FFs and to the modeling of excited hadronic states.

The paper is organized as follows: The formalism is developed in Sec. II and some of the kinematical constraints for the considered reactions are discussed in Sec. III. Section IV contains a discussion on nucleon FFs and of our choices of parametrization, for electromagnetic as well as for axial FFs. In Sec. V the numerical results for the differential cross section of the considered processes will be presented. In Sec. VI we discuss the results and summarize the perspectives opened by the experimental study of these reactions, including possible manifestation of heavy (radial) excited π states.

II. FORMALISM

Let us consider reactions (1) and (2) and calculate the corresponding matrix elements in the framework of a phenomenological approach based on Compton-like Feynman amplitudes. The Feynman diagrams for reaction (1) are shown in Figs. 1(a) and 1(b) for pair emission from the proton and from the antiproton, respectively. For reaction (2), the corresponding Feynman diagrams are shown in Figs. 2(a), 2(b), and 2(c) for pair emission from the charged pion, from the antiproton, and from the neutron, respectively.

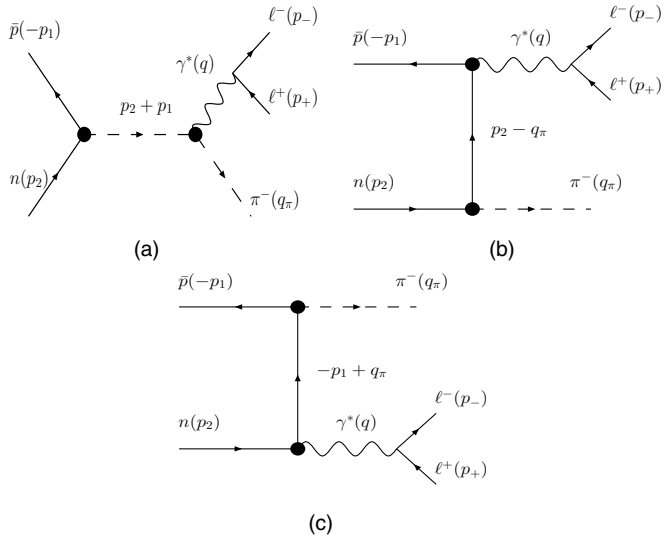

FIG. 2. Feynman diagrams for the reaction $\bar{p}+n \to \pi^- + \ell^+ + \ell^-$.

As previously discussed in Ref. [2], no free nucleons are involved in the electromagnetic vertices of pions and nucleons, as one of the hadrons is virtual, and rigorously speaking, the form factors involved should be modified by taking into account off-mass-shell effects. However, we will use the expression for electromagnetic current involving on-mass-shell hadrons. A discussion of the errors and the consequences of such approximation is given below.

The vertices $\gamma^* \bar{N}\bar{N}^* \to \gamma^* \bar{N}\bar{N}$ and $\gamma^*\pi\pi \to \gamma^*\pi\pi^*$ contain information on the electromagnetic FFs of protons, neutrons, and pions (with the FFs of antiprotons differing by sign from proton FFs, owing to charge symmetry requirements). Nucleon FFs can be expressed in terms of Dirac and Pauli FFs, $F_{1,2}^{p,n}(q^2)$, which enter in the expression of the electromagnetic current:

$$\begin{aligned}&\langle N(p')|\Gamma_\mu(q)^N|N(p)\rangle \\ &\quad = \bar{u}(p')\left[F_1^N(q^2)\gamma_\mu + \frac{F_2^N(q^2)}{4M}(\hat{q}\gamma_\mu - \gamma_\mu\hat{q})\right]u(p), \\ &N = n,\, p,\end{aligned} \tag{3}$$

where M is the nucleon mass, q is the four-momentum of the virtual photon, and $\hat{q} = q_\nu\gamma_\nu$. The nucleon FFs in the kinematical region of interest for the present work are largely unexplored. The assumptions and the parametrizations used for FFs in the numerical applications are detailed in the following.

The pion electromagnetic FF, $F_\pi(q^2)$, is also introduced in the standard way. The corresponding current has the form

$$J_\mu^\pi = (q_1+q_2)_\mu F_\pi\left(q_\pi^2\right), \tag{4}$$

with q_1 and q_2 the ingoing and outgoing charged pion momenta, and $q_\pi = q_1 - q_2$. Special attention must be devoted to the pion-nucleon interaction in the vertices $\pi N\bar{N}$, which are parametrized as

$$\bar{v}(p_1)\gamma_5 u(p_2) g_{\pi NN}(s) \quad \text{and} \quad \bar{v}(p_1-q)\gamma_5 u(p_2) g_{\pi NN}\left(m_\pi^2\right), \tag{5}$$

with $s = (p_1+p_2)^2$. The vertex of the πNN interaction is related to the general axial vector current matrix element:

$$\begin{aligned}&\langle N(p')|A_j^\mu(0)|N(p)\rangle \\ &\quad = \bar{u}(p')\left[G_A(q^2)\gamma_\mu + \frac{q^\mu}{2M}G_P(q^2) + i\frac{\sigma^{\mu\nu}}{2M}G_T(q^2)\right] \\ &\qquad \times \gamma_5\frac{\tau_j}{2}u(p),\end{aligned} \tag{6}$$

where $q_\mu = p'_\mu - p_\mu$, $G_A(q^2)$ is the axial nucleon FF, $G_P(q^2)$ is the induced pseudoscalar FF, and $G_T(q^2)$ is the induced pseudotensor FF. In the chiral limit, the requirement of conservation of the axial current leads to the relation

$$4M^2 G_A(q^2) + q^2 G_P(q^2) = 0, \tag{7}$$

which shows that $G_P(q^2)$ has a pole at small q^2. Indeed, assuming that the axial current interacts with the nucleon through the conversion to the pion interaction, one obtains

$$G_P(q^2) = -\frac{4Mf_\pi g_{\pi NN}(q^2)}{q^2}. \tag{8}$$

Comparing Eqs. (7) and (8) one obtains the Goldberger-Treiman relation

$$\frac{G_A}{f_\pi} = \frac{g_{\pi NN}}{M}. \tag{9}$$

We suggest a generalization of this relation in the form

$$\begin{aligned}g(s) &= g_{\pi\bar{N}N}(s) = \frac{\mathrm{M}G_A(s)}{f_\pi}, \\ G_A(0) &= 1.2673 \pm 0.0035,\end{aligned} \tag{10}$$

where $g(s)$ and $g(m_\pi^2)$ are the pion-nucleon coupling constants for pions off and on the mass shell. This assumption can be justified by the fact that f_π is weakly dependent on q^2 and it is in agreement with the ChPT expansion at small q^2 [16]. Therefore measuring the $g_{\pi\bar{N}N}(s)$ coupling constant gives information on the axial and induced pseudoscalar FFs of the nucleon in the chiral limit (neglecting the pion mass).

The matrix element is expressed in terms of the hadronic H and leptonic J currents:

$$\begin{aligned}M^i &= \frac{4\pi\alpha}{q^2}H_\mu^i J^\mu(q), \quad H_\mu^i = \bar{v}(p_1)O_\mu^i u(p_2), \\ J^\mu(q) &= \bar{v}(p_+)\gamma_\mu u(p_-),\end{aligned} \tag{11}$$

where the index $i = 0, -$ refers to π^0 and π^-, respectively. The cross section for the case of unpolarized particles has a standard form [if we take the nucleon target (proton or neutron) to be at rest in the laboratory frame]:

$$d\sigma^i = \frac{1}{16PM}\sum|M^i|^2 d\Gamma, \quad P^2 = E^2 - M^2, \tag{12}$$

where E (P) is the energy (the modulus of the momentum) and $d\Gamma$ is the phase space volume given by

$$d\Gamma = \frac{1}{(2\pi)^5}\frac{d^3p_+}{2\epsilon_+}\frac{d^3p_-}{2\epsilon_-}\frac{d^3q_\pi}{2E_\pi} \times \delta^4(p_1+p_2-p_+-p_--q_\pi). \quad (13)$$

The phase space volume can be written as

$$d\Gamma = \frac{d^3q_\pi}{2E_\pi}d\Gamma_q\frac{d^4q}{(2\pi)^5}\delta^4(p_1+p_2-q-q_\pi),$$

with

$$d\Gamma_q = \frac{d^3p_+}{2\epsilon_+}\frac{d^3p_-}{2\epsilon_-}\delta^4(q-p_+-p_-).$$

Considering an experimental setup where the pion four-momentum is fully measured, we can perform the integration on the phase space volume of the lepton pair:

$$\int d\Gamma_q \sum J_\mu(q)J_\nu^*(q) = -\frac{2\pi}{3}(q^2+2\mu^2)\beta\Theta(q^2-4\mu^2) \times \left(g_{\mu\nu}-\frac{q_\mu q_\nu}{q^2}\right), \quad (14)$$

where Θ is the usual step function, μ is the lepton mass, and $\beta=\sqrt{1-(4\mu^2/q^2)}$.

The cross section can be expressed in the form

$$d\sigma^i = \frac{\alpha^2}{6s\pi r}\frac{\beta(q^2+2\mu^2)}{(q^2)^2}\mathcal{D}^i\frac{d^3q_\pi}{2\pi E_\pi}, \quad (15)$$

with

$$s=(q_\pi+q)^2=2M(M+E), \quad r=\sqrt{1-(4M^2/s)}, \quad (16)$$

and

$$\mathcal{D}^i = \left(g_{\mu\nu}-\frac{q_\mu q_\nu}{q^2}\right)\frac{1}{4}\mathrm{Tr}(\hat{p}_1-M)O_\mu^i(\hat{p}_2+M)\left(O_\nu^i\right)^*, \quad i=0,-. \quad (17)$$

Using Feynman rules we can write (see Figs. 1 and 2)

$$O_\mu^- = \Gamma_\mu^p(q)\frac{\hat{p}_1-\hat{q}-M}{(p_1-q)^2-M^2}\gamma_5 g\left(m_\pi^2\right) - \gamma_5\frac{\hat{p}_2-\hat{q}+M}{(p_2-q)^2-M^2}\Gamma_\mu^n(q)g\left(m_\pi^2\right) + \frac{(2q_\pi+q)_\mu}{s-m_\pi^2}g(s)F_\pi(q^2)\gamma_5, \quad (18)$$

$$O_\mu^0 = \Gamma_\mu^p(q)\frac{\hat{p}_1-\hat{q}-M}{(p_1-q)^2-M^2}\gamma_5 g\left(m_\pi^2\right) - \gamma_5\frac{\hat{p}_2-\hat{q}+M}{(p_2-q)^2-M^2}\Gamma_\mu^p(q)g\left(m_\pi^2\right). \quad (19)$$

Note that the hadronic current $\mathcal{J}_\mu^0 = \bar{v}(p_1)O_\mu^0 u(p_2)$ is conserved ($J_\mu^0 q^\mu = 0$), but $J_\mu^- = \bar{v}(p_1)O_\mu^- u(p_2)$ is not conserved:

$$q_\mu\mathcal{J}_\mu^- = \left[\left(-F_1^p(q^2)+F_1^n(q^2)\right)g\left(m_\pi^2\right)+g(s)F_\pi(q^2)\right] \times \bar{v}(p_1)\gamma_5 u(p_2) = \mathcal{C}\bar{v}(p_1)\gamma_5 u(p_2). \quad (20)$$

Therefore, to provide gauge invariance, it is necessary to add to O_μ^- a contact term with the appropriate structure [Eq. (20)]. The explicit expressions for $\mathcal{D}^0$ and $\mathcal{D}^-$ are given in the Appendix.

Selecting the coefficients that depend on pion energy in $\mathcal{D}_i$, Eq. (17), we can perform an analytical integration on the pion energy. In the limit of small lepton pair invariant mass, q^2, after integration on pion energy, the differential cross section with respect to q^2 becomes

$$(q^2)^2\left.\frac{d\sigma}{dq^2}\right|_{q^2\ll M^2} \simeq \frac{\alpha^2\left[g(s)-g\left(m_\pi^2\right)\right]^2}{24\pi r}. \quad (21)$$

Equation (21) contains one of the most important results of this work, as it shows that the measurement of the cross section at small q^2 allows one to experimentally determine the off-mass-shell pion-nucleon coupling constant.

Writing the differential cross section in the form

$$\frac{d\sigma}{dq^2} = \frac{(q^2+2\mu^2)\beta}{(q^2)^2}\left[\frac{c}{q^2}+R(q^2)\right], \quad (22)$$

with c and $R(0)$ finite functions of s, and integrating over the lepton invariant mass, we find

$$\sigma_{\mathrm{tot}} = \int_{4\mu^2}^{s}\frac{d\sigma}{dq^2}dq^2 = \frac{c(s)}{5\mu^2}+R(0,s)\left(\log\frac{s}{\mu^2}-\frac{5}{3}\right) + \int_0^s\frac{dq^2}{q^2}[R(q^2,s)-R(0,s)]. \quad (23)$$

The first term in the right-hand side of Eq. (23) is divergent for massless leptons, and it induces a rise of the cross section (especially in the case of electron-positron pair). However, it is very hard to experimentally achieve such kinematics ($q^2\to 4\mu^2$). The total cross section can be integrated within the experimental limits of detection of the particles. Such (partial) total cross section will be calculated in the following.

III. KINEMATICS

In the laboratory system, useful relations can be derived among the kinematical variables that characterize the reaction. The allowed kinematical region at a fixed incident total energy s can be illustrated as a function of different useful variables.

One can find the following relation between q^2, the invariant mass of the lepton pair, and the pion energy:

$$q^2 = (p_1+p_2-q_\pi)^2 = 2M^2+m_\pi^2+2M(E-E_\pi) - 2p_1q_\pi = s+m_\pi^2-2E_\pi M-2p_1q_\pi, \quad (24)$$

with

$$2p_1q_\pi = 2E_\pi E-2\sqrt{E_\pi^2-m_\pi^2}P\cos\theta_\pi, \quad (25)$$

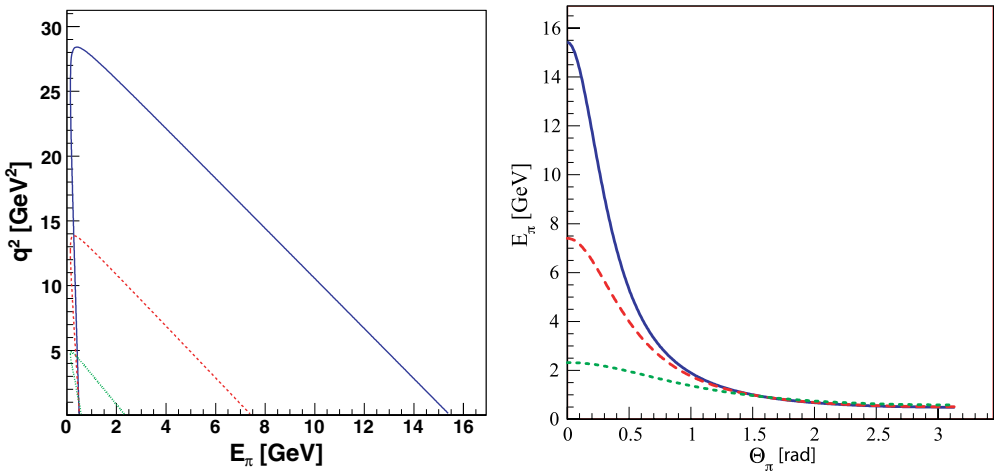

FIG. 3. (Color online) (Left) The kinematical limit for q^2 for $\cos\theta_\pi = -1$ and for $\cos\theta_\pi = 1$ in the lab system as a function of the pion energy for different values of the beam energy: $E = 2$ GeV (dotted line), $E = 7$ GeV (dashed line), and $E = 15$ GeV (solid line). The allowed kinematical region lies below the curves. (Right) Kinematical limit for the pion energy E_π as a function of the pion angle (lab system) for $E = 2$ GeV (dotted line), $E = 7$ GeV (dashed line), and $E = 15$ GeV (solid line) for the minimum value of $q^2 \simeq m_\pi^2$.

where $\theta_\pi = \widehat{\vec{p}_1\vec{q}_\pi}$ is the angle between the antiproton and the pion momenta (in the laboratory frame).

The limit $-1 \leqslant \cos\theta_\pi \leqslant 1$ translates into maximal and minimal values for the pion energy. The allowed kinematical region is shown in Fig. 3 (left) for three values of the beam energy: $E = 2$, 7, and 15 GeV. To this constraint, one should add the minimal thresholds $q^2 \geqslant 4m_\ell^2$ and $E_\pi \geqslant m_\pi$. For the minimal value of $q^2 \simeq m_\pi^2$, one can plot the dependence of the pion energy on θ_π [Fig. 3 (right)] for different values of the beam energy. As the energy increases the kinematically allowed region becomes wider. At backward angles the maximum pion energy becomes larger at small s values. For larger values of q^2, E_π is smaller.

For fixed values of the lepton pair invariant mass, the pion energy can take values in the region

$$\frac{E_\pi^{\min}}{M} = \frac{s-q^2}{s(1+r)} \leqslant \frac{E_\pi}{M} \leqslant \frac{s-q^2}{s(1-r)} = \frac{E_\pi^{\max}}{M}, \qquad (26)$$

if we neglect the pion mass.

We can write the phase space volume of the produced pion (neglecting terms $\simeq m_\pi^2/m_N^2$) in three (equivalent) forms:

$$\begin{aligned}\frac{d^3q_i}{2\pi E_\pi} &= dq^2\delta[q^2 - 2E_\pi(E + M - P\cos\theta_\pi)] \\ &\quad \times E_\pi dE_\pi d\cos\theta_\pi \\ &= E_\pi dE_\pi d\cos\theta_\pi \qquad (27a) \\ &= M\frac{dq^2}{sr}dE_\pi \qquad (27b) \\ &= \frac{q^2M^2dq^2d\cos\theta_\pi}{s^2(1-r\cos\theta_\pi)^2}. \qquad (27c)\end{aligned}$$

IV. AXIAL AND ELECTROMAGNETIC FORM FACTORS

Experimental measurements on FFs are the object of ongoing programs in several world facilities. Hadron FFs are measured in the space-like (SL) region through elastic electron hadron scattering and in the time-like (TL) region through annihilation reactions. It has been only recently possible to use polarization techniques. The availability of high-intensity, high-energy polarized beams allows these measurements to be extended to large-q^2 regions and the achievement of very high precision.

The theoretical effort for a complete description of the nucleon structure should be extended to a unified picture that applies to the full kinematical region (SL and TL) [18]. Few phenomenological models developed for the SL region can be successfully extended to the TL region [19]. A tentative extrapolation of a TL model to the SL region has also been done, and constraints have been found from the few available data [12].

In the TL region, data for electromagnetic FFs exist over the NN threshold, up to 18 GeV^2 [20], but a precise separation of the electric and magnetic contributions has not yet been possible, owing to the low statistics. Moreover, FFs are complex quantities, and polarization experiments are necessary to determine their relative phase. Presently only the moduli of FFs are available, under the hypothesis $|G_E^N|^2 = |G_M^N|^2$ or $G_E^N = 0$. These data have been obtained in the reactions $e^+ + e^- \leftrightarrow \bar{p} + p$ (see Ref. [21] and references therein) and, more recently, by the radiative return method [22], in the region over the kinematical threshold $s > 3.52$ GeV^2. The possible existence of an $N\bar{N}$ resonance under threshold has also been predicted as an explanation of the fact that TL FFs are larger than SL ones at corresponding $|q^2|$ values. To give quantitative predictions, for the cross section of processes (1) and (2), it is necessary to know the value of FFs in the unphysical region. As data are not available, such estimation can be only done in the framework of models based, for example, on Vector Meson Dominance (VMD) or on dispersion relations, which predict several discontinuities from meson resonances. Not all nucleon models give expressions for FFs that can be extended to the TL region, and not all nucleon models give a satisfactory description of all four nucleon FFs.

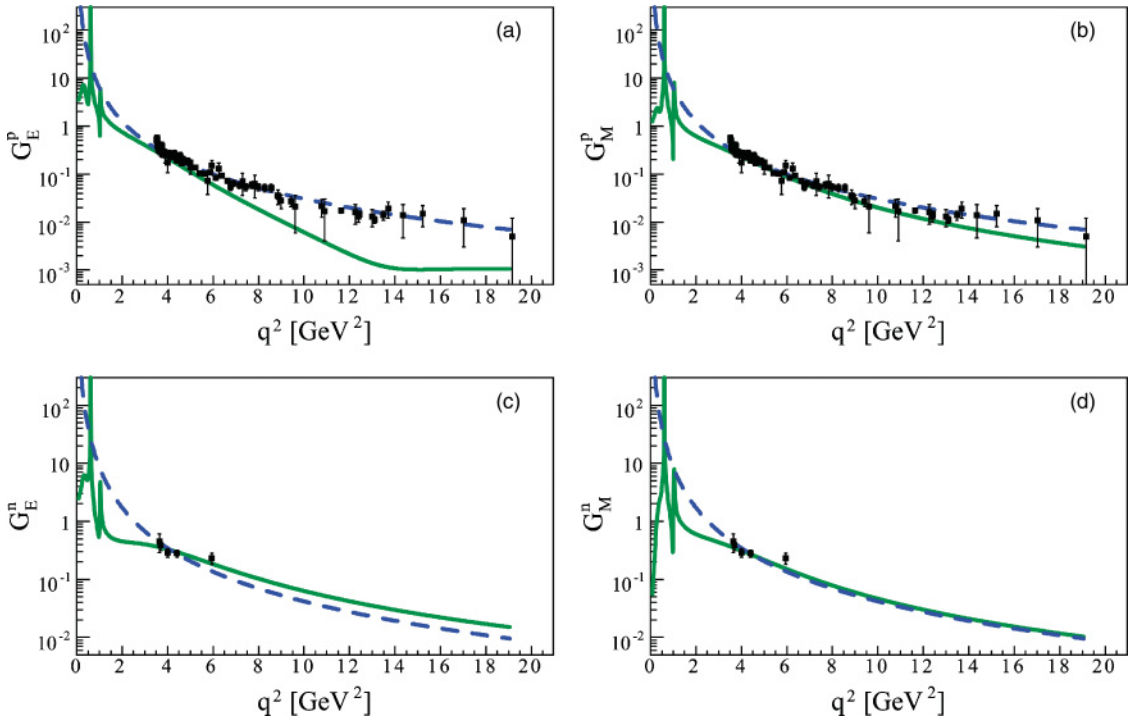

FIG. 4. (Color online) Nucleon electromagnetic FFs in the time-like region: proton electric FF (a), proton magnetic FF (b), neutron electric FF (c), and neutron magnetic FF (d). Data are from Ref. [22] and predictions of the model [23] (solid line) and from pQCD (dashed line).

Following Ref. [19], in the present calculation we use two models for electromagnetic FFs. The first was a model based on Ref. [23], which first predicted the behavior of the proton electric FF as found from recent polarization experiments [7] and recently extended to the TL region. This model, as with all VMD-inspired models, has poles in the unphysical region, in correspondence with the meson resonances that are taken into account. To have a smooth parametrization, we also considered a model inspired by the perturbative QCD (pQCD) prescription (corrected by dispersion relations [24]), which reproduces the experimental data in the TL region but does not show discontinuities and can be considered an "average" expectation:

$$\left|G_E^N\right| = \left|G_M^N\right| = \frac{A(N)}{q^4\left(\ln^2\frac{q^2}{\Lambda^2} + \pi^2\right)}, \quad q^2 > \Lambda^2, \quad (28)$$

where $\Lambda = 0.3$ GeV is the QCD scale parameter and A is fitted to the data. This parametrization is taken to be the same for the proton and the neutron. The best fit is obtained with parameters $A(p) = 98$ GeV^4 for the proton and $A(n) = 134$ GeV^4 for the neutron, which reflects the fact that, in the TL region, neutron FFs are systematically larger than those for the proton. In principle, this parametrization holds only for very large q^2 values, but, in practice, it reproduces the existing data quite well in the whole physical region. Evidently, it is meaningless at small q^2 ($q^2 < \Lambda^2$), and it has poor normalization properties for $q^2 \to 0$.

Usually the data are shown in terms of the Sachs FFs, electric G_E^N, and magnetic G_M^N, which are related to the Pauli and Dirac FFs by the following relations:

$$G_E^N = F_1^N + F_2^N, \quad G_M^N = F_1^N + \tau F_2^N, \quad \tau = q^2/(4M^2).$$

They correspond in a nonrelativistic limit or (in the Breit frame) to the Fourier transform of the charge density (electric form factor G_E) and magnetization distribution (magnetic form factor G_M) of the proton.

The behavior of these FFs compared with the existing experimental data is shown in Fig. 4. For the neutron, the first and still unique measurement in the TL region was done at Frascati by the FENICE Collaboration [25].

For the pion FF, a reasonable description exists in the kinematical region of interest here; for a recent discussion see Ref. [26]. For the sake of simplicity, we use here a ρ-meson-saturated monopole-like parametrization, which takes

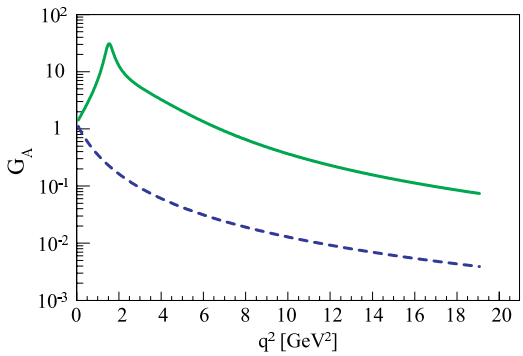

FIG. 5. (Color online) Proton axial FF from VMD-inspired model (solid line) and from a dipole extrapolation (dashed line).

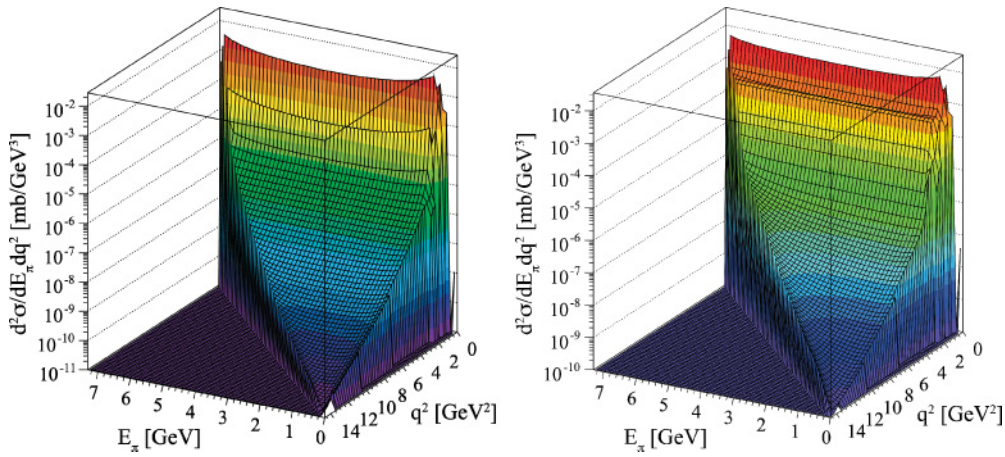

FIG. 6. (Color online) (Left) Double differential cross section for the reaction $\bar{p} + p \to \pi^0 + \ell^+ + \ell^-$ as a function of q^2 and E_π, using FFs from Ref. [23] for the nucleon and Eq. (31) for the axial FF. (Right) Same quantity as in the left plot but for the reaction $\bar{p} + n \to \pi^- + \ell^+ + \ell^-$. The kinematical constraints in the (E_π, q^2)-plane shown in Fig. 3 are visible here.

a Breit Wigner form in the TL region:

$$F_\pi(q^2) = \frac{m_\rho^2}{m_\rho^2 - q^2 - i m_\rho \Gamma_\rho}. \tag{29}$$

Data on axial FFs in the TL region do not exist, and they suffer in the SL region from a model-dependent derivation. In the SL region, the nucleon axial FF, $G_A(q^2)$, for the transition $W^* + p \to n$ (where W^* is the virtual W boson), can be described by the following simple formula [27]:

$$G_A(q^2) = G_A(0)(1 - q^2/m_A^2)^{-n} \tag{30}$$

with $m_A = 1.06$ GeV, if $n = 2$. A simple analytical continuation of this prescription to the the TL region presents a pole in the unphysical region. Therefore we used a "mirror" parametrization from the SL region:

$$FF^{(\mathrm{TL})}(|q^2|) = FF^{(\mathrm{SL})}(|q^2|).$$

Such a prescription is, in principle, valid only at very large q^2, since it obeys asymptotic analytical properties of FFs [18].

For comparison, another parametrization (inspired from Ref. [23]) is also used [28]:

$$G_A^{\mathrm{SL}}(q^2) = d(q^2) G_A(0) \left[1 - \alpha + \alpha \frac{m_A^2}{m_A^2 - q^2}\right]. \tag{31}$$

Here the parameter $\alpha = 1.893 \pm 0.02$ has been fitted to the available data, in the SL region, by averaging the dispersion from the model-dependent extraction of the data themselves, $m_A \simeq 1.235$ GeV is the mass of a light axial meson, and $d(q^2) = (1 - \gamma q^2)^{-2}$ is the function describing the internal core of the nucleon. We take γ as a fixed parameter, from the fit of nucleon electromagnetic form factors: $\gamma \simeq 0.25\ \mathrm{GeV}^{-2}$. Let us note however that this value is not good from a t-channel point of view, because it gives a pole in the physical region, $t_0 = \frac{1}{\gamma} = 4\ \mathrm{GeV}^{-2}$. To extend the expression (31) to the TL region, following Ref. [23], we add a phase to the dipole term. Moreover, the complex nature of the axial FF is ensured

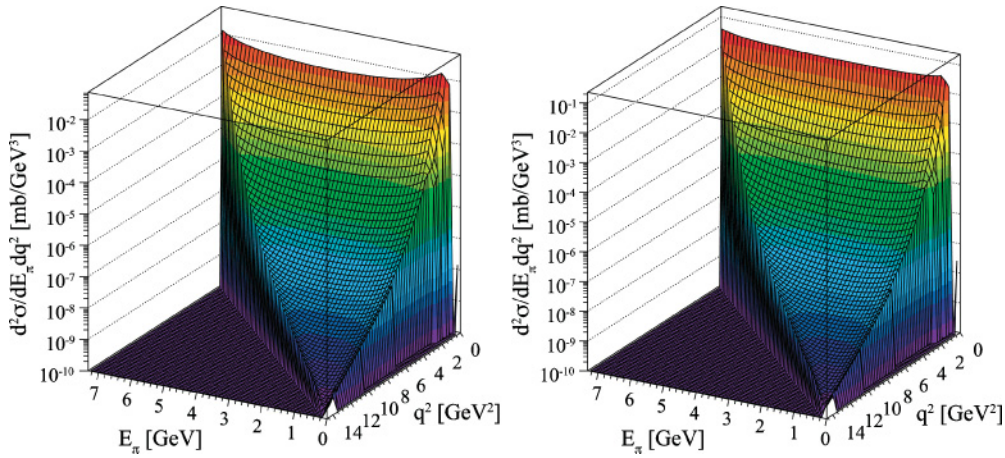

FIG. 7. (Color online) (Left) Double differential cross section for the reaction $\bar{p} + p \to \pi^0 + \ell^+ + \ell^-$ as a function of q^2 and E_π, using pQCD-inspired nucleon FFs and dipole axial FFs. (Right) Same quantity as in the left plot but for the reaction $\bar{p} + n \to \pi^- + \ell^+ + \ell^-$.

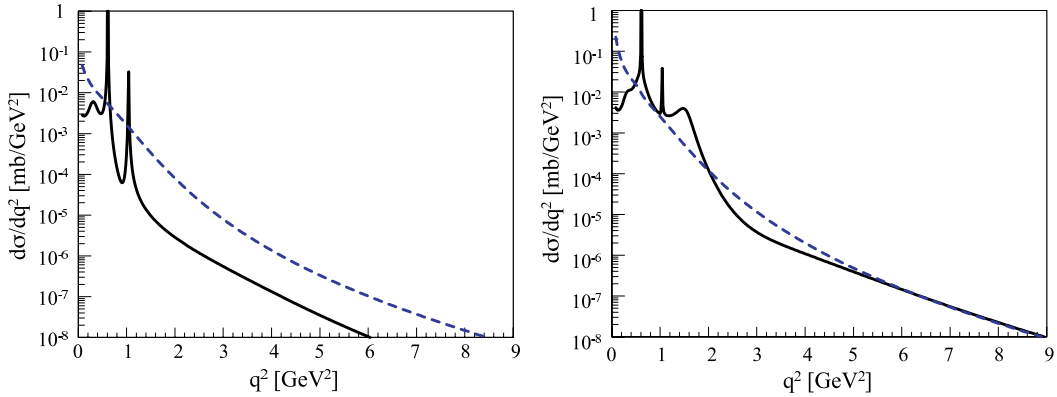

FIG. 8. (Color online) (Left) Differential cross section for the process $\bar{p} + p \to \pi^0 + \ell^+ + \ell^-$ as a function of q^2, with FFs from Ref. [23] for the nucleon and Eq. (31) for the axial FF (solid line) and with FFs from pQCD-inspired nucleon FFs and dipole axial FFs (dashed line). (Right) Same quantity as in the left plot but for the reaction $\bar{p} + n \to \pi^- + \ell^+ + \ell^-$.

by adding a width to the axial meson, and we replace the propagator as in Eq. (29).

The expression for the TL axial FF therefore becomes

$$G_A(q^2) = d(q^2) G_A(0) \left[1 - \alpha + \alpha \frac{m_A^2}{m_A^2 - q^2 - i m_A \Gamma_A} \right], \tag{32}$$

with $d(q^2) = (1 - \gamma e^{i\delta} q^2)^{-2}$, where $\Gamma_A = 0.140$ GeV and $\delta = 0.925$.

The two models for G_A used in the calculation of the cross section are shown in Fig. 5 and differ by one order of magnitude. Moreover, an enhancement is expected from Eq. (32), in correspondance to the mass of the axial meson.

V. RESULTS

The differential and integrated cross sections were calculated for several values of the antiproton energy and the different choices of FFs just described.

The differential cross sections, Eq. (15), as a function of E_π and q^2, Eq. (27a), are shown in Figs. 6 and 7 for the reactions $\bar{p} + p \to \pi^0 + \ell^+ + \ell^-$ and $\bar{p} + n \to \pi^- + \ell^+ + \ell^-$ at $E = 7$ GeV. As one can see from the figures, the differential cross sections are large and measurable in a wide range of the considered variables. It is reasonable to assume that the region up to $q^2 = 7$ GeV^2, at least, will be accessible by the experiments at FAIR.

The discontinuities in the small-q^2 regions are smoothed out by the steps chosen to histogram the variables. However, depending on the resolution and the reconstruction efficiency, it will be experimentally possible to identify the meson and nucleon resonances.

The differential cross section as a function of q^2 can be obtained after integrating on the pion energy, Eq. (15), with the help of Eq. (27b):

$$\frac{d\sigma^i}{dq^2} = \frac{\alpha^2}{6 s \pi r} \frac{\beta(q^2 + 2\mu^2)}{(q^2)^2} \frac{M}{sr} \int_{E_{\pi\min}}^{E_{\pi\max}} \mathcal{D}^i \, dE_\pi, \tag{33}$$

where the integration on the hadronic term is detailed in the Appendix. The result of the calculation is shown in Fig. 8. For charged pion production, the presence of the axial FF is the

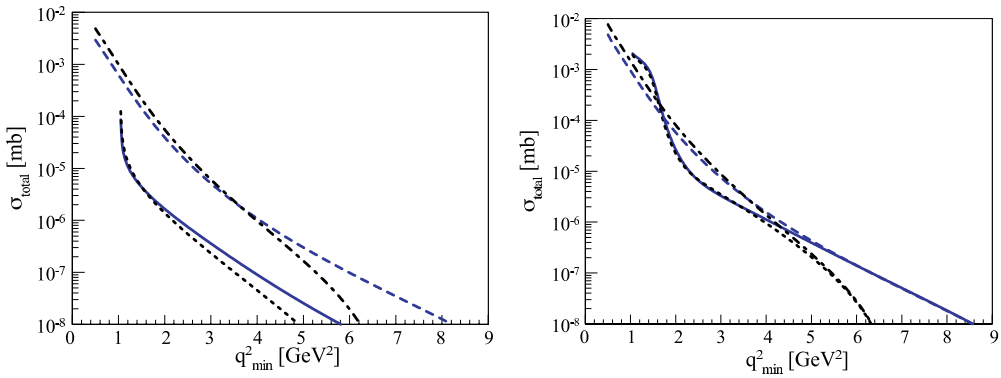

FIG. 9. (Color online) (Left) Total cross section for the process $\bar{p} + p \to \pi^0 + \ell^+ + \ell^-$ as a function of $q_{\min}$ for different values of s and different FFs: dotted (solid) line for $E = 7\,(12)$ GeV, nucleon FFs from Ref. [23] and axial FF from Eq. (31); dash-dotted (dashed) line for $E = 7\,(12)$ GeV, pQCD-inspired nucleon FFs and dipole axial FFs. (Right) Same quantity as in the left plot but for the process $\bar{p} + n \to \pi^- + \ell^+ + \ell^-$.

reason for the larger cross section as compared to the neutral pion case. For both reactions, again, the present calculation gives an integrated cross section of the order of several μb in the unphysical region for both choices of FFs.

The q^2 dependence is driven by the choice of FFs. For the pQCD-like FFs, the behavior is smooth and similar for both protons and neutrons. For the FFs from Ref. [23], the resonant behavior owing to ρ, ω, and ϕ poles appears in the figures. The partial total cross section, integrated over q^2, Eq. (23), is shown in Fig. 9, as a function of $q_{\min} \gg 4\mu^2$ for two different values of $s, s = 2$ and 5 GeV^2. Evidently, the calculations for the VMD FFs [23] have been done beyond the resonance region, as a result of the divergence of the integrals at the meson poles.

Let us estimate the uncertainties inherent to our model assumptions. The off-mass-shell effects were previously discussed for these particular reactions in Ref. [2]. A considerable theoretical effort has been devoted to this problem in the past (see Ref. [29] and references therein), and it was shown that indeed off-mass-shell effects can be large and lead to an increase in FFs. In the region of virtuality, $p^2 \leqslant 0.5$ GeV^2, it was calculated that off-mass-shell effects modify FFs at the level of 3%. The Q^2 dependence of FFs is not changed significantly, when one of the particles goes off shell. It is interesting to note that the ratio of electric to magnetic nucleon FFs is rather insensitive to off-shell effects. Moreover, ChPT arguments [30] support a smooth behavior of FFs as a function of the degree of nucleon virtuality $\delta \sim |\frac{p^2-M^2}{M^2}|^2 \leqslant 2$, which does not exceed 10%. For the present kinematics the virtuality involved varies in the interval $2m_\pi/M < \delta < 2 - 2m_\pi/M$. In the case of detection of soft pions in the laboratory frame, errors arising from off-shell effects will decrease to 3–5%. These considerations support an estimation on the precision of our model at the level of 10%.

In the intermediate state, in principle, the Δ resonance or other resonances can be excited. The calculation of the contribution of the Δ resonance is largely model dependent and will be the object of specific considerations.

VI. CONCLUSION AND PERSPECTIVES

The differential cross section for the processes $\bar{p} + n \to \pi^- + \ell^- + \ell^+$ and $\bar{p}+p \to \pi^0+\ell^-+\ell^+$ has been calculated in the kinematical range that will be accessible in the near future at FAIR. The main interest of these reactions is related to the possibility of measuring nucleon electromagnetic and axial FFs in the time-like and the unphysical regions. As previously pointed out [1,2], varying the momentum of the emitted pion allows one to scan the q^2 region of interest, keeping the beam energy fixed.

In Ref. [2] it was also noticed that, in the lepton invariant mass squared distribution, a divergent term was present:

$$\frac{d\sigma}{dq^2} \simeq \frac{[2F_1^v(q^2) + F_\pi(q^2)]^2}{(q^2)^2}, \quad q^2 \to 0, \tag{34}$$

where in our notation the right-hand side of Eq. (34) corresponds to $\mathcal{C}^2/(q^2)^2$. It was argued that the singularity at $q^2 \to 0$ cancels because $2F_1^v(0) = 1$ and $F_\pi(0) = -1$. This compensation takes place if $g_{\pi\bar{N}N}(s) = g_{\pi\bar{N}N}(m_\pi^2)$ holds, which is verified for annihilation at rest. In the present work, one cannot rely on such an assumption and the validity of this relation has to be verified experimentally.

The detailed measurement of the double differential cross section, as a function of q^2 and E_π, in principle allows us to extract all nucleon FFs that are involved in the considered reactions. A precise simulation of the different processes involving the production of a pion will be necessary along with a study of the best kinematical conditions to minimize background contribution. In particular, the reaction $\bar{p} + p \to \pi^0+\pi^0$ has been identified as a potential source of background in the e^+e^--spectrum because of its Dalitz decay, $\pi^0 \to e^+e^-\gamma$.

The assumption about the validity of a generalized form of the Goldberger-Treiman relation, which allows the pseudoscalar $g_{\pi NN}$ coupling constant to be related to the axial nucleon FF, can be experimentally verified for small invariant mass of the lepton pair. In the process of π^- production, it is in principle possible to study heavy negatively charged pions, as the π' resonance of mass $M' = 1300$ MeV, which is interpreted as a radial excitation of pion. The matrix element for the excitation of a resonant state for the virtual charged pion in the intermediate state, $M_{\rm res}$, can be written as follows:

$$M_{\rm res} = \frac{4\pi\alpha}{q^2} \frac{g_{\pi N\bar{N}}}{s - M'^2 + iM'\Gamma'} \bar{v}(p_1)\gamma_5 u(p_2)\lambda(q^2) \times \left(q_\mu - \frac{q^2}{qq_\pi} q_{\pi\mu}\right) J_\mu. \tag{35}$$

The corresponding cross section is

$$d\sigma_{\rm res} = \frac{\alpha^2}{12r\pi} \frac{|\lambda(q^2) g_{\pi N\bar{N}}|^2}{(s - M'^2)^2 + M'^2\Gamma'^2} \frac{d^3q_\pi}{2\pi E_\pi}, \tag{36}$$

where $\lambda(q^2)$ is the transition from factors for the vertex $\pi'\pi\gamma^*$. We do not consider processes involving vector mesons, Δ resonances, and higher excited nucleon states. Their contribution can be estimated in frame of models and will be the object of further considerations.

In case of multipion production, the quantity $s_1 = (p_1 + p_2 - q)^2 - m_\pi^2$ becomes positive. By varying s_1 at fixed beam energy, by changing q^2 and θ_π, it is in principle possible to identify and study other mechanisms, such as the excitation of heavy pion resonances, π', or the possible presence of a $N\bar{N}$ "quasi-deuteron" state under the kinematical threshold for $p\bar{p}$ annihilation in two leptons. The study of multipion production will be the subject of a forthcoming publication.

ACKNOWLEDGMENTS

The authors are thankful to L. Lipatov for critical remarks on the manuscript and interesting discussions. Useful discussions with S. Scherer, H. W. Hammer, and G. I. Gakh are acknowledged. Two of us (E.A.K. and C.A.) are grateful to DAPNIA/SPhN, Saclay, where this work was done. The Slovak Grant Agency for Sciences VEGA is acknowledged by C.A. for support under Grant No. 2/4099/26.

APPENDIX

In this appendix we give the explicit expression of the coefficients entering in the calculation of the cross section, as well as useful integrals.

Let us define q^2-dependent terms, which contain FFs and the necessary constants:

$$\begin{aligned} f_a(s) &= F_\pi(q^2) G_{\pi N \bar{N}}(s), \quad f_{iN}(q^2) = g\left(m_\pi^2\right) F_i^N(q^2), \\ i &= 1, 2, \quad N = n, p, \\ \mathcal{C}(s) &= f_a(s) - f_{1p}(q^2) + f_{1n}(q^2), \end{aligned}$$

and the quantity

$$X = \frac{p_1 q_\pi}{p_2 q_\pi} = (s - q^2)/(2M E_\pi) - 1. \tag{A1}$$

Let us write the expressions for the hadronic part of the matrix element (17): For the process $p + \bar{p} \to \ell^+ + \ell^- + \pi^0$

$$\begin{aligned} \mathcal{D}^0 &= \left|f_{2p}\right|^2 \left[\frac{E - M}{M} - \frac{1}{2}\left(1 - \frac{q^2}{4M^2}\right)\frac{(1 - X)^2}{X}\right] \\ &\quad + \left|f_{1p} - f_{2p}\right|^2 \frac{(X + 1)^2}{X}. \end{aligned} \tag{A2}$$

For the process $n + \bar{p} \to \ell^+ + \ell^- + \pi^-$

$$\begin{aligned} \mathcal{D}^- &= \frac{1}{4}\left[\sum_i C_{i,i} |f_i|^2 + 2 \sum_{j,k;j<k} C_{j,k} \mathrm{Re}(f_j f_k^*) \right. \\ &\quad \left. + \frac{2|\mathcal{C}|^2 s}{q^2}\right], i, j, \\ k &= 1p, 2p, 1n, 2n, a. \end{aligned} \tag{A3}$$

The explicit expressions of the coefficients are

$$\begin{aligned} C_{1p,1p} &= 4X, \quad C_{2p,2p} = \frac{s}{M^2}\left(1 + \frac{q^2}{2s} X\right), \\ C_{1p,2p} &= -3(1 + X), \quad C_{a,a} = \frac{2q^2}{s} - 4, \\ C_{1n,1n} &= 4\frac{1}{X}, \quad C_{2n,2n} = \frac{s}{M^2}\left(1 + \frac{q^2}{2sX}\right), \\ C_{1n,2n} &= -3\left(1 + \frac{1}{X}\right), \quad C_{a,1p} = 2, \\ C_{a,2p} &= \left(1 - \frac{q^2}{s}\right)(1 + X), \quad C_{1p,1n} = 4, \\ C_{1p,2n} &= \left(\frac{1}{X} - 2X - 1\right), \\ C_{2p,2n} &= \left(2 + \frac{2}{X} - \frac{q^2}{2M^2} + X\right), \\ C_{2p,1n} &= \left(X - \frac{2}{X} - 1\right), \quad C_{a,1n} = -2, \\ C_{a,2n} &= -\left(1 - \frac{q^2}{s}\right)\left(1 + \frac{1}{X}\right). \end{aligned} \tag{A4}$$

The structure of $\mathcal{D}_i$ allows us to select the terms that depend on the pion energy. It is straightforward to perform an analytical integration on the pion energy by using the following integrals:

$$\int_{E_\pi^{\min}}^{E_\pi^{\max}} \frac{dE_\pi}{M} = \frac{r(s - q^2)}{2M^2} = rb, \quad b = \frac{s - q^2}{2M^2}; \tag{A5}$$

$$\begin{aligned} \int_{E_\pi^{\min}}^{E_\pi^{\max}} \frac{dE_\pi}{M} X &= \int_{E_\pi^{\min}}^{E_\pi^{\max}} \frac{dE_\pi}{M} \frac{1}{X} = \frac{s - q^2}{2M^2}\left[\ln\frac{1 + r}{1 - r} - r\right] \\ &= b(\ell - r), \end{aligned} \tag{A6}$$

with r given in Eq. (16) and $\ell = \ln[(1 + r)/(1 - r)]$. The result of the integration on the pion energy is the following: For the process $p + \bar{p} \to \ell^+ + \ell^- + \pi^0$

$$\begin{aligned} \int_{E_\pi^{\min}}^{E_\pi^{\max}} \mathcal{D}^0 \frac{dE_\pi}{M} &= b\left\{2\left|f_{1p} - f_{2p}\right|^2 \ell + \left|f_{2p}\right|^2 \right. \\ &\quad \left. \times \left[\frac{E - M}{M} r + \left(1 - \frac{q^2}{4M^2}\right)(2r - \ell)\right]\right\} \end{aligned} \tag{A7}$$

and for the process $p + \bar{p} \to \ell^+ + \ell^- + \pi^0$

$$\begin{aligned} \int_{E_\pi^{\min}}^{E_\pi^{\max}} \mathcal{D}^- \frac{dE_\pi}{M} &= \frac{b}{4}\left[\sum_i K_{i,i} |f_i|^2 + 2 \sum_{j,k;j<k} K_{j,k} \right. \\ &\quad \left. \times \mathrm{Re}(f_j f_k^*) + |\mathcal{C}|^2 \frac{2rs}{q^2}\right], \end{aligned} \tag{A8}$$

where

$$\begin{aligned} K_{1p,1p} &= 4(\ell - r), \quad K_{2p,2p} = \frac{s}{M^2}\left(r + \frac{q^2}{2s}(\ell - r)\right), \\ K_{1p,2p} &= -3\ell, \quad K_{a,a} = \left(\frac{2q^2}{s} - 4\right) r, \\ K_{1n,1n} &= 4(\ell - r), \quad K_{2n,2n} = \frac{s}{M^2}\left(r + \frac{q^2}{2s}(\ell - r)\right), \\ K_{1n,2n} &= -3\ell, \quad K_{a,1p} = 2r, \quad K_{a,2p} = \left(1 - \frac{q^2}{s}\right)\ell, \\ K_{1p,1n} &= 4r, \quad K_{1p,2n} = -\ell, \\ K_{2p,2n} &= \left[3\ell - \left(1 + \frac{q^2}{2M^2}\right) r\right], \quad K_{2p,1n} = -\ell, \\ K_{a,1n} &= -2r, \quad K_{a,2n} = -\left(1 - \frac{q^2}{s}\right)\ell. \end{aligned} \tag{A9}$$

[1] M. P. Rekalo, Sov. J. Nucl. Phys. **1**, 760 (1965).
[2] A. Z. Dubnickova, S. Dubnicka, and M. P. Rekalo, Z. Phys. C **70**, 473 (1996).
[3] P. Spiller and G. Franchetti, Nucl. Instrum. Methods Phys. Res. A **561**, 305 (2006); see also http://www.gsi.de/fair/
[4] R. Hofstadter, F. Bumiller, and M. Yearian, Rev. Mod. Phys. **30**, 482 (1958).
[5] J. Friedrich and Th. Walcher, Eur. Phys. J. A **17**, 607 (2003).
[6] A. I. Akhiezer and M. P. Rekalo, Sov. Phys. Dokl. **13**, 572 (1968) [Dokl. Akad. Nauk Ser. Fiz. **180**, 1081 (1968)]; A. I. Akhiezer and M. P. Rekalo, Sov. J. Part. Nucl. **4**, 277 (1974) [Fiz. Elem. Chast. Atom. Yad. **4**, 662 (1973)].
[7] M. K. Jones *et al*., Phys. Rev. Lett. **84**, 1398 (2000); O. Gayou *et al*., *ibid*. **88**, 092301 (2002); V. Punjabi *et al*., Phys. Rev. C **71**, 055202 (2005) [Erratum-*ibid*. **71**, 069902 (2005)].
[8] R. C. Walker *et al*., Phys. Rev. D **49**, 5671 (1994); L. Andivahis *et al*., *ibid*. **50**, 5491 (1994); I. A. Qattan *et al*., Phys. Rev. Lett. **94**, 142301 (2005).
[9] Yu. M. Bystritskiy, E. A. Kuraev, and E. Tomasi-Gustafsson, Phys. Rev. C **75**, 015207 (2007); E. Tomasi-Gustafsson, arXiv:hep-ph/0610108.
[10] P. G. Blunden, W. Melnitchouk, and J. A. Tjon, Phys. Rev. C **72**, 034612 (2005); A. V. Afanasev, S. J. Brodsky, C. E. Carlson, Y. C. Chen, and M. Vanderhaeghen, Phys. Rev. D **72**, 013008 (2005); P. A. M. Guichon and M. Vanderhaeghen, Phys. Rev. Lett. **91**, 142303 (2003).
[11] H. W. Hammer and U.-G. Meissner, Eur. Phys. J. A **20**, 469 (2004).
[12] R. Baldini, C. Bini, P. Gauzzi, M. Mirazita, M. Negrini, and S. Pacetti, Eur. Phys. J. C **46**, 421 (2006).
[13] J. Haidenbauer, H.-W. Hammer, U. G. Meissner, and A. Sibirtsev, Phys. Lett. **B643**, 29 (2006).
[14] V. Bernard, N. Kaiser, and U. G. Meissner, Int. J. Mod. Phys. E **4**, 193 (1995).
[15] S. Scherer and J. H. Koch, Nucl. Phys. **A534**, 461 (1991).
[16] T. Fuchs and S. Scherer, Phys. Rev. C **68**, 055501 (2003).
[17] V. Bernard, N. Kaiser, and U. G. Meissner, Int. J. Mod. Phys. E **4**, 193 (1995).
[18] E. Tomasi-Gustafsson and M. P. Rekalo, Phys. Lett. **B504** 291 (2001).
[19] E. Tomasi-Gustafsson, F. Lacroix, C. Duterte, and G. I. Gakh, Eur. Phys. J. A **24**, 419 (2005).
[20] M. Ambrogiani *et al*. (E835 Collaboration), Phys. Rev. D **60**, 032002 (1999).
[21] J. Z. Bai *et al*. (BES Collaboration), Phys. Rev. Lett. **91**, 022001 (2003).
[22] B. Aubert *et al*. (BABAR Collaboration), Phys. Rev. D **73**, 012005 (2006).
[23] F. Iachello, A. D. Jackson, and A. Lande, Phys. Lett. **B43**, 191 (1973); F. Iachello, arXiv:nucl-th/0312074; F. Iachello and Q. Wan, Phys. Rev. C **69**, 055204 (2004).
[24] D. V. Shirkov and I. L. Solovtsov, Phys. Rev. Lett. **79**, 1209 (1997); Theor. Math. Phys. **150**, 132 (2007).
[25] A. Antonelli *et al*., Nucl. Phys. **B517**, 3 (1998).
[26] C. Bruch, A. Khodjamirian, and J. H. Kuhn, Eur. Phys. J. C **39**, 41 (2005).
[27] V. Bernard, L. Elouadrhiri, and U. G. Meissner, J. Phys. G **28**, R1 (2002).
[28] E. A. Kuraev, C. Adamuscin, E. Tomasi-Gustafsson, and F. Maas, DAPNIA-06-450, 2006.
[29] H. W. L. Naus and J. H. Koch, Phys. Rev. C **36**, 2459 (1987); **39**, 1907 (1989).
[30] Ulf-G. Meissner (private communication).